Available online at www.sciencedirect.com

ScienceDirect

Developmental Biology 298 (2006) 470–484

DEVELOPMENTAL BIOLOGY

www.elsevier.com/locate/ydbio

Genetic manipulation of blood group carbohydrates alters development and pathfinding of primary sensory axons of the olfactory systems

James A. St John [a], Christina Claxton [a], Mark W. Robinson [a], Fumiichiro Yamamoto [b], Steven E. Domino [d], Brian Key [a,c,*]

[a] *Brain Growth and Regeneration Laboratory, School of Biomedical Sciences, The University of Queensland, Brisbane 4072, Queensland, Australia*
[b] *The Burnham Institute, La Jolla Cancer Research Center, La Jolla, CA 92037, USA*
[c] *Centre for Functional and Applied Genomics, The University of Queensland, Brisbane, 4072, Queensland, Australia*
[d] *Department of Obstetrics and Gynecology, University of Michigan Medical Center, Ann Arbor, MI 48109, USA*

Received for publication 7 April 2006; revised 29 June 2006; accepted 30 June 2006
Available online 7 July 2006

Abstract

Primary sensory neurons in the vertebrate olfactory systems are characterised by the differential expression of distinct cell surface carbohydrates. We show here that the histo-blood group H carbohydrate is expressed by primary sensory neurons in both the main and accessory olfactory systems while the blood group A carbohydrate is expressed by a subset of vomeronasal neurons in the developing accessory olfactory system. We have used both loss-of-function and gain-of-function approaches to manipulate expression of these carbohydrates in the olfactory system. In null mutant mice lacking the α(1,2)fucosyltransferase FUT1, the absence of blood group H carbohydrate resulted in the delayed maturation of the glomerular layer of the main olfactory bulb. In addition, ubiquitous expression of blood group A on olfactory axons in gain-of-function transgenic mice caused mis-routing of axons in the glomerular layer of the main olfactory bulb and led to exuberant growth of vomeronasal axons in the accessory olfactory bulb. These results provide in vivo evidence for a role of specific cell surface carbohydrates during development of the olfactory nerve pathways.

Keywords: Carbohydrate; Blood group A; Blood group H; Neuron; Guidance; Glomerulus; Accessory olfactory

Introduction

The mammalian olfactory topographic map is characterized by the mosaic distribution of primary olfactory neurons throughout regions of the olfactory neuroepithelium lining the nasal cavity (Ressler et al., 1994; Strotmann et al., 1994a,b; Vassar et al., 1993). A remarkable sorting of axons occurs as they project from the neuroepithelium to their targets in the olfactory bulb. In the mouse, primary olfactory neurons express one of approximately 1000 different odorant receptors and their axons project to topographically fixed positions in the olfactory bulb (Nagao et al., 2000; Ressler et al., 1994; Vassar et al., 1994). The sorting of these axons en route to their target appears to involve the coordinated spatiotemporal expression of both adhesion molecules and guidance receptors. While NCAM is ubiquitously expressed and probably non-selectively promotes axon growth (Aoki et al., 1999; Treloar et al., 1997), the cell adhesion molecule OCAM is restricted to a large subpopulation of axons that specifically terminates in the ventrolateral olfactory bulb (Alenius and Bohm, 1997; Gussing and Bohm, 2004; Nagao et al., 2000; Yoshihara et al., 1997). Further sorting appears to be regulated by the more restricted expression of ephrin-As (Cutforth et al., 2003), Neuropilin-1 (Pasterkamp et al., 1998), Neuropilin-2 (Cloutier et al., 2002; Walz et al., 2002), galectin-1 (Puche et al., 1996) and the odorant receptors themselves.

Despite the contribution of these molecules, it is still unclear how the primary olfactory axons achieve the precision of glomerular targeting observed in this sensory system. The

* Corresponding author. Brain Growth and Regeneration Laboratory, School of Biomedical Sciences, The University of Queensland, Brisbane 4072, Queensland, Australia. Fax: +61 7 3365 1299.
E-mail address: brian.key@uq.edu.au (B. Key).

0012-1606/$ - see front matter © 2006 Elsevier Inc. All rights reserved.
doi:10.1016/j.ydbio.2006.06.052

potential exists for other, as yet unidentified, axon guidance molecules to contribute to the fine-tuning of olfactory axon navigation. Cell surface carbohydrates have intriguing expression patterns on discrete subpopulations of primary sensory axons in both the main and accessory olfactory systems (Allen and Akeson, 1985; Dowsing et al., 1997; Fujita et al., 1985; Key and Giorgi, 1986; Lipscomb et al., 2002, 2003; Pays and Schwarting, 2000; Salazar and Sanchez Quinteiro, 2003; Schwarting and Crandall, 1991; Schwarting et al., 1992; St John and Key, 2001; St John and Key, 2002).

We hypothesized that the selective expression of cell surface carbohydrates by sensory axons is pivotal for the normal development of the olfactory nerve pathway (see review by Key and St John, 2002). One of the predictions of this hypothesis is that manipulation of the complement of cell surface carbohydrates will perturb axon growth and guidance. Genetic manipulation of the composition of cell surface carbohydrates is one strategy to examine the role of these molecules in the development of the olfactory system. While knockout of a large range of lactosamine carbohydrates has recently been reported, this resulted in widespread death of primary olfactory neurons and therefore subsequent poor innervation of the olfactory bulb (Henion et al., 2005). What is now needed is more specific targeting of carbohydrate manipulation so that neurons survive and their axons project to the olfactory bulb.

Some of the cell surface carbohydrates are present on unique glycoforms of NCAM and have been identified as blood group epitopes. The blood group H (BGH) carbohydrate (αFuc(1,2) Gal) is recognised by the lectin *Ulex europaeus* agglutinin-I and is expressed by primary olfactory neurons and their axons in mice (Ducray et al., 1999; Lipscomb et al., 2002, 2003; Salazar and Sanchez Quinteiro, 2003). BGH is the acceptor substrate for glycosyltransferases that synthesize the blood group A (BGA) epitope by addition of terminal *N*-acetyl-D-galactosamine. BGA is expressed by subpopulations of primary olfactory neurons in rat (Astic et al., 1989; Mollicone et al., 1985; Pays and Schwarting, 2000) while in the developing mouse, BGA is present on a subpopulation of vomeronasal organ (VNO) axons that terminate in a unique caudal zone of the accessory olfactory bulb (St. John and Key, unpublished data).

We postulated that the sugars present on NCAM were involved in axon–target recognition in the olfactory system. To examine the role of these sugars, we first examined loss-of-function mice which lacked the α(1,2)fucosyltransferase FUT1 that synthesizes BGH (Domino et al., 2001a). In these mice, there was delayed maturation of the nerve fibre and glomerular layers of the main olfactory bulb. Despite loss of the BGH in the accessory olfactory bulb of these mice there were no observable defects in targeting of accessory axons, suggesting that expression of other carbohydrates and axon guidance molecules were sufficient for this behaviour. We therefore examined the effect of gain-of-function of carbohydrates by genetically engineering the expression of the human blood group A glycosyltransferase (BGAT) (Yamamoto and McNeill, 1996) on all olfactory sensory neurons in transgenic mice using the promoter for olfactory marker protein (OMP) (Danciger et al., 1989). In these transgenic mice, VNO axons overshot their target and projected into deeper inappropriate lamina in the accessory olfactory bulb. Mis-routing errors were also observed in the glomerular layer of the main olfactory bulb in these mice. Together, these data suggest that blood group sugars are involved in axon guidance events in the developing olfactory systems.

Materials and methods

Generation of FUT1 and FUT2 deficient mice

Mice lacking most of the coding regions of either the FUT1 or FUT2 fucosyltransferase genes were generated as previously described (Domino et al., 2001a). Both targeting vectors used to make these deletions led to the insertion of the *E. Coli* β-galactosidase coding sequence in frame to the remaining amino terminal domains of FUT1 and FUT2. Histochemical staining for β-galactosidase revealed the expression pattern of these genes in tissue sections of the nasal cavity.

Generation of BGAT transgenic mice

Transgenic mice expressing the human blood group A glycosyltransferase (BGAT) in sensory neurons of the main and accessory olfactory systems were generated. In these mice, referred to as BGAT-Tg, the full length (5.5 kb) olfactory marker protein (OMP) promoter (Danciger et al., 1989) drove the expression of the human histo-blood group A transferase (Yamamoto and McNeill, 1996) in all primary and accessory olfactory neurons. The 1.062 kb coding sequence of BGAT was amplified using a forward primer containing sequence from the *Aat*II site (within the 5′ UTR of OMP) to the start site. A Kpn site was incorporated into the reverse primer directly after the stop signal. The 1.93 kb *Aat*II/Kpn fragment of OMP was then replaced with the amplified coding sequence of BGAT. The OMP promoter containing the BGAT reporter was excised from vector sequences by digestion with *Not*1/*Eco*R1, purified and then injected into mouse oocytes at the Transgenic Animal Service of Queensland (University of Queensland, Brisbane). Transgenic lines were established by genotype analysis using PCR with primers specifically designed for the blood group A glycosyltransferase transgene: 5′AACCTCAGCTTCCTCGGAC3′ and 5′TGAAGCTGTTCCTGGAGA3′. Genotyping was further confirmed by immunohistochemistry using antibodies against the BGA carbohydrate. BGAT-Tg animals were separately crossed with M72-IRES-tau:GFP mice (Potter et al., 2001), V1rb2-GFP mice (Rodriguez et al., 1999) and with V2r1b-GFP mice (Del Punta et al., 2002). All procedures were carried out with the approval of, and in accordance with, the University of Queensland Animal Ethics Experimentation Committee and the Commonwealth Office of the Gene Technology Regulator.

Animal preparation

Late postnatal and adult mice were killed by CO_2 asphyxiation; embryos and early postnatal mice were killed by decapitation. Heads were immersion fixed overnight at 4°C in 4% paraformaldehyde in phosphate buffered saline (PBS; pH 7.4). Mice were genotyped by polymerase chain reaction (PCR) with genomic DNA isolated from mouse tails and the genotype was confirmed by immunohistochemistry for BGA. Following fixation, adult heads were decalcified in 20% disodium ethylene diaminetetraacetic acid in PBS (pH 7.4). Heads were placed in embedding matrix (O.C.T. compound, Miles Scientific, Naperville, IL) and snap frozen by immersion in iso-pentane that had been cooled by liquid nitrogen. For wholemount preparations of V1rb2-GFP and V2r1b-GFP mice, fluorescent images were taken of unfixed tissue.

Histochemistry

Cryostat sections (30 μm) of embryonic and post-natal animals were cut, mounted on to gelatinized slides and stored at − 20°C. Sections were incubated with 0.15% H_2O_2 in methanol for 5 min before being washed with 0.1 M Tris buffered saline (TBS, pH 7.4) and 0.3% Triton-X-100 (TX-100) for 2 min. They

were then incubated with 2% bovine serum albumin (BSA; Sigma Chemical Corporation) in 0.1 M TBS with 0.3% Triton X-100 for 30 min at room temperature (RT). The sections were incubated overnight at 4°C with primary antibodies in 2% BSA and 0.3% TX-100 in TBS. Primary antibodies used were (1) murine monoclonal antiserum against BGA (neat, CSL Limited, Parkville, Victoria, Australia), (2) murine monoclonal antiserum against BGB (neat, CSL Limited), (3) goat polyclonal antiserum against OMP (1:10,000) (Keller and Margolis, 1975). Sections were then washed with TBS/Triton-X-100 before the appropriate secondary antibodies were added: biotinylated goat anti-mouse immunoglobulin antibodies (1:200, Vector Laboratories Inc., Burlingame, CA) or biotinylated rabbit anti-goat immunoglobulin antibodies (1:400, Vector Laboratories Inc). Sections were incubated for 1 h at RT, washed in TBS/Triton X-100 and then incubated with avidin–biotin–horseradish peroxidase (Vector Laboratories Inc) for 1 h at RT. Following a wash in TBS, staining was visualized by reaction with 3,3′-diaminobenzidine (DAB) and hydrogen peroxide (H_2O_2) in TBS. Sections were then dehydrated in ethanol, cleared in xylene and cover-slipped with DPX mounting medium.

For double label immunohistochemistry, sections were incubated overnight at 4°C with goat polyclonal antiserum against OMP and murine monoclonal antibodies against BGA. The sections were washed with TBS and TX-100 and then incubated in rabbit anti-goat immunoglobulin antibody conjugated to biotin (1:200; Vector Laboratories, Inc, CA, USA) for 1 h at RT. The sections were then incubated for 1 h at RT with mouse anti-IgM antibodies and with streptavidin, each conjugated to fluorescein or Texas red (1:50, Vector), before being washed and coverslipped with fluorescent mounting medium. Images of the sections were captured by confocal laser scanning microscopy (MRC 1024, Bio-Rad Laboratories Inc., Hercules, CA) using an Olympus BX60 microscope or with an Olympus BX51 compound fluorescence microscope. Serial optical sections were imaged at 2 μm intervals and were projected to give a two-dimensional reconstruction.

For lectin staining, sections were incubated with (1) biotinylated *Ulex europaeus* agglutinin-I (1:50, Sigma) or (2) biotinylated *Bandeiraea simplicifolia* lectin I isolectin B4 (1:50, Sigma), in BSA/TBS/Triton X-100 with 1.25 mM $CaCl_2$, 1.25 mM $MgCl_2$ and 1.25 mM $MnCl_2$. The sections were then washed in TBS/Triton X-100, incubated with avidin–biotin–horseradish peroxidase for 1 h at RT and staining visualized by reaction with diaminobenzidine as described above.

Images were collected using a SPOT 2e Digital Camera (Spot Diagnostic Instruments Inc.) attached to an Olympus BH2-RFCA microscope fitted with differential interference contrast optics, under the control of SPOT imaging software. Images were then compiled in Adobe Photoshop 7.0 and Adobe Illustrator 10.0 (Adobe Systems Incorporated).

DiI injections

Whole heads of P2.5 wild type ($n=7$) and BGAT-Tg ($n=5$) were fixed in 4% PFA for 3 days. 1,1′-dioctodecyl-3,3,3′,3′-tetramethylindocarbocyanine perchlorate (DiI) (Molecular Probes, Eugene, Oregon, USA) was injected into each VNO using a micro-injection needle. The injected heads were immersed in 4% PFA for 1 week before they were re-injected with DiI. Specimens were then placed in the dark in 4% PFA for 9 weeks. Sagittal sections (100 μm) of the brains were cut on a Campden Instruments Motorized Advance MA752 Vibroslice and stored in 4% PFA in twenty-four well plates in the dark. Some sections were stained with the nucleic acid stain, Acridine Orange (1 in 10^6; Molecular Probes). Images of the sections were captured by confocal laser scanning microscopy (MRC 1024, Bio-Rad Laboratories Inc.) using an Olympus BX60 microscope. Serial optical sections were imaged at 2 μm intervals and were projected to give a two-dimensional reconstruction.

Quantification of staining density

As an indirect comparison of the level of BGAT expression, the density of anti-BGA immunostaining was quantified. Sections were immunostained using the same protocol and diaminobenzidine reaction time, and photographed using identical microscope and camera settings. The density of staining over a randomly selected fixed area was quantified using Image-Pro Plus version 5.0 (MediaCybernetics, Silver Spring, MD). Statistical significance was assessed using a two-tailed *t*-test.

Quantification of Fut1$^{-/-}$ mutant mice

Quantification of the changes in size of anatomical structures was performed on coronal sections of Fut1$^{-/-}$ that were OMP immunostained, with measurements taken every 240 μm along the rosto-caudal axis; accessory olfactory bulb analyses were performed on sagittal sections. Distance measurements were made using Spot imaging software (Spot Diagnostic Instruments). The average thickness of nerve fibre layer (NFL) was made at the most ventral portion of NFL and mid way up the medial surface of the NFL on both bulbs of $n=6$ animals. Thickness of the neuroepithelium lining both sides of the septum was measured at the dorsal septum in $n=3$ animals. The sizes of the olfactory bulbs and accessory olfactory bulbs were determined by counting the number of sections from rostral to caudal and by measuring the maximum coronal cross-sectional area of both olfactory bulbs in $n=6$ animals. The number of glomeruli along the medial surface of both the left and right olfactory bulbs was counted over a 500 μm distance in $n=6$ animals; as was the number of glomeruli with a diameter greater than 30 μm. The number of neurons in the neuroepithelium lining the left and right septum was counted along 150 μm of the dorsal septum in $n=3$ animals.

Quantification of over-projecting axons

The number of over-projecting axons labeled with DiI was counted in every section of accessory olfactory bulb. The number of over-projecting axons stained by anti-BGA immunohistochemistry was counted in every second section of accessory olfactory bulb in P21 wild type ($n=5$) and BGAT-Tg ($n=8$) animals. The six longest axons in both P21 wild type ($n=4$) and BGAT-Tg ($n=4$) animals were measured using SPOT imaging software (Spot Diagnostic Instruments Inc.) and the mean length for each animal was calculated. Statistical significance was assessed using the Wilcoxon rank sum test.

Results

FUT1 is essential for blood group H carbohydrate synthesis in the olfactory systems

The histo blood group H (BGH) carbohydrate, which was detected by lectin staining using *Ulex europeaus* agglutinin I (UEA-I), was selectively expressed by primary sensory axons in the developing olfactory system. BGH was first observed at E12.5 and by P2.5 strong expression was evident throughout the nerve fibre and glomerular layers of both the main and accessory olfactory bulbs (Fig. 1A). The BGH antigen is synthesized by the action of either of two different α(1,2) fucosyltransferase enzymes, FUT1 or FUT2 (Domino et al., 1997, 2001b), each of which catalyses the addition of fucose to an acceptor substrate carbohydrate (Fig. 1C). To determine the active FUT enzyme in the olfactory system we examined the previously generated FUT1$^{-/-}$ and FUT2$^{-/-}$ null mutant mice (Domino et al., 2001a) for expression of BGH. In the FUT1$^{-/-}$ mice, BGH was not expressed by primary sensory axons in either the main or accessory olfactory bulb (Fig. 1B), whereas in FUT2$^{-/-}$ mice, BGH expression was similar to control mice (data not shown). These results are consistent with the expression of FUT1 by olfactory and vomeronasal sensory neurons as determined by staining for β-galactosidase (not shown). The FUT1 null mice have the *E. Coli* β-galactosidase coding region inserted in the FUT1 locus. Hence FUT1 is the enzyme responsible for generating the BGH carbohydrate in primary sensory neurons of the main and accessory olfactory systems.

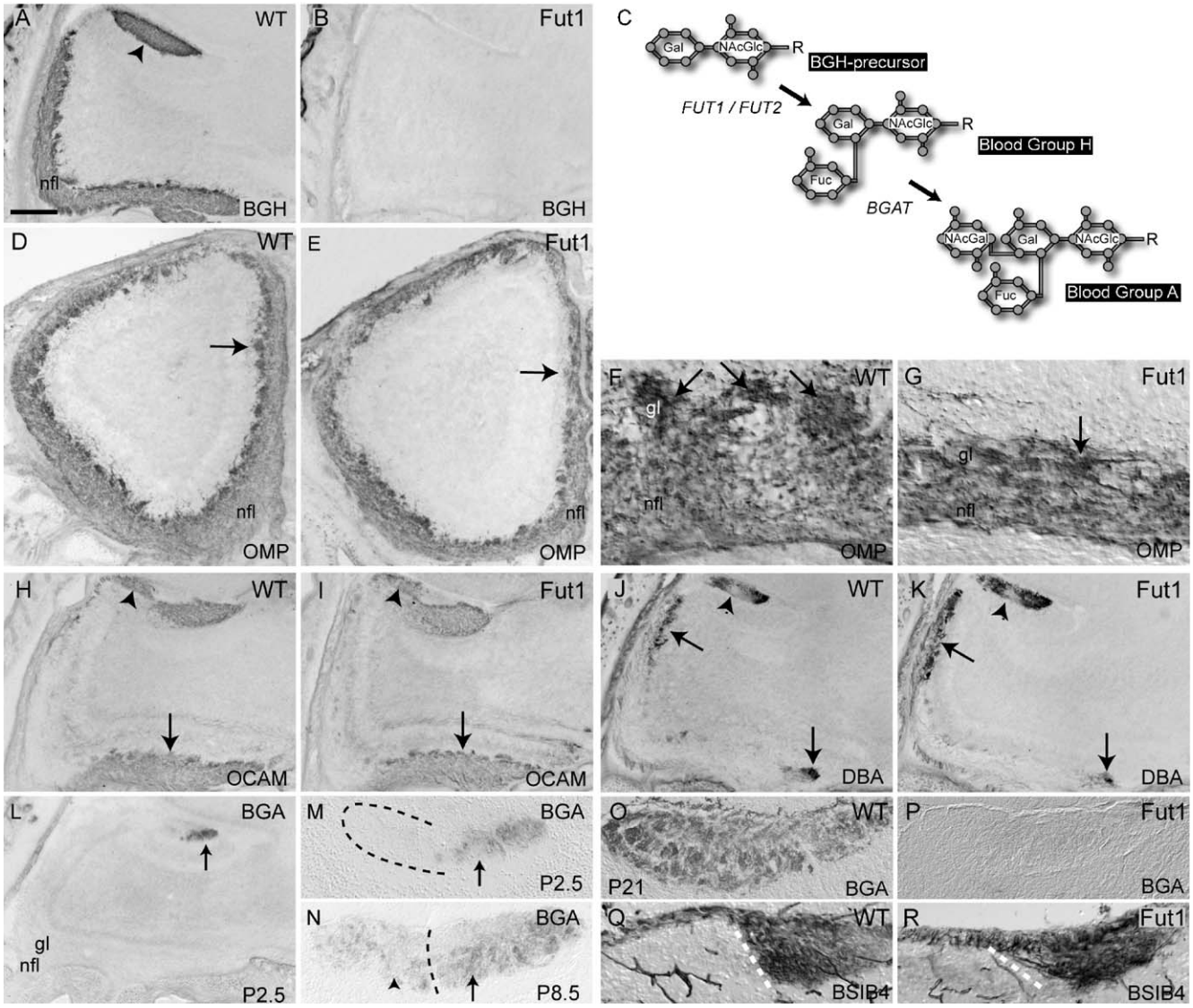

Fig. 1. Loss of Blood Group H carbohydrate affects olfactory development. Panels D–G are coronal sections of wild type and FUT1$^{-/-}$ knockout mice; all other panels are parasagittal sections with rostral to the left and dorsal to the top. (A) In P1.5 wild type mice, BGH is expressed by primary sensory axons throughout the main and accessory (arrow) olfactory bulb. (B) In FUT1$^{-/-}$ mice, BGH is not expressed. (C) The Blood Group H precursor carbohydrate is synthesized into BGH by the enzyme FUT1 or FUT2; BGH is then modified by Blood Group A glycosyltransferase (BGAT) to synthesize BGA carbohydrate. (D) OMP immunohistochemistry in P1.5 wild type mice; distinct glomeruli (arrow) are visible throughout the main olfactory bulb; higher power view of the medial NFL is shown in (F), arrows show glomeruli. (E) In P1.5 FUT1$^{-/-}$ mice, the nerve fibre layer (nfl) on the medial and ventral surfaces is reduced and glomeruli are smaller and less distinct (arrow); higher power view of the medial NFL is shown in (G), arrow shows presumptive glomeruli. (H) OCAM immunohistochemistry in wild type P1.5 mice reveals staining in the ventral main olfactory bulb (arrow) and rostral accessory olfactory bulb (AOB) (arrowhead). Sensory axons in the caudal AOB are not stained. (I) OCAM expression is unaffected in FUT1$^{-/-}$ mice. (J) DBA lectin histochemistry in P1.5 wild type mice stains subpopulations of axons in the main olfactory bulb (arrows) and in the AOB with the characteristic low level staining in the central accessory olfactory bulb (arrowhead). (K) DBA histochemistry is unaffected in FUT1$^{-/-}$ mice. (L) In P2.5 mice, BGA is expressed by a subpopulation of primary sensory axons (arrow) that terminate in the caudal accessory olfactory bulb (AOB). Primary olfactory axons present in the nerve fibre and glomerular layers (nfl and gl) in the main olfactory bulb do not express BGA. (M) Higher power view of the AOB. BGA axons terminate in discrete glomeruli (arrow) in the caudal AOB and do not enter the rostral AOB (dashed region). (N) At P8.5, BGA expression is more widespread in the caudal AOB (arrow) and is also present in the rostral AOB (arrowhead). The rostro-caudal division is shown by the dashed line. (O) By P21, BGA expression is uniformly strong across the entire AOB. (P) BGA is absent in FUT1$^{-/-}$ mice. (Q) The lectin BSI-B4 stains the caudal AOB in P1.5 wild type mice; dashed line indicates rostral-caudal division. (R) BSI-B4 staining is unaffected in FUT1$^{-/-}$ mice. Scale bar is 250 μm in panels A, B, H–K; 200 μm in panels D, E; 30 μm in panels F, G; 160 μm in panel L; 40 μm in panel M; 65 μm in panels N, Q, R; 130 μm in panels O, P.

Loss of blood group H affects primary olfactory development

In order to assess the role of BGH in growth and development of primary sensory axons in the olfactory system we next examined the formation of the olfactory nerve fibre and glomerular layers in the olfactory bulbs of neonatal FUT1$^{-/-}$ and control mice. Olfactory marker protein (OMP) immunostaining was used to selectively label primary olfactory axons in coronal sections of the olfactory bulbs of the postnatal day 1.5 (P1.5) old animals (Figs. 1D–G). At low magnification, the

olfactory nerve fibre and glomerular layers appeared thinner in the FUT1$^{-/-}$ mice (Figs. 1D, E). This was particularly noticeable along the ventromedial surface of the main olfactory bulb. When viewed at higher magnification, many glomeruli were smaller and not demarcated from the nerve fibre layer as in the control animals (Figs. 1F, G). The thickness of the nerve fibre layer was quantified and found to be 20% smaller on the ventral surface (Fut1$^{-/-}$ mice = 68.4 ± 8.5 μm; control mice = 85.3 ± 4.1 μm; $p < 0.05$, $n = 12$ bulbs in 6 animals) and 24% smaller on the medial surface (Fut1$^{-/-}$ mice = 36.3 ± 2.9 μm; control mice = 47.5 ± 3.4 μm; $p < 0.01$; $n = 12$ bulbs in 6 animals) of the bulb compared to controls. In addition, FUT1$^{-/-}$ mice had 21% fewer glomeruli on the medial surface of the main olfactory bulb than control mice (Fut1$^{-/-}$ mice = 5.4 ± 0.4 glomeruli per 500 μm; control mice = 6.9 ± 0.5 glomeruli per 500 μm; $p < 0.05$, $n = 12$ bulbs in 6 animals). In order to determine the effect of loss of FUT1 on the size of glomeruli we counted the number of glomeruli with a diameter greater than 30 μm. In control mice, 60% of glomeruli on the medial surface had a diameter greater than 30 μm at P1.5. In comparison FUT1$^{-/-}$ mice had 38% fewer glomeruli with a diameter greater than 30 μm than control mice (Fut1$^{-/-}$ mice = 2.6 ± 0.4 glomeruli per 500 μm; control mice = 4.3 ± 0.5 glomeruli per 500 μm; $p < 0.01$, $n = 12$ bulbs in 6 animals). Despite the reduction in nerve fibre layer thickness and glomeruli number and size there were no observed difference either in the overall size of the olfactory bulbs, in the thickness of the olfactory neuroepithelium, or in the number of primary neurons within the neuroepithelium between FUT1$^{-/-}$ and control mice at P1.5. Interestingly, the reduction in the thickness of the nerve fibre layer and in the number and size of glomeruli was transient. By 3 weeks of age there was no detectable difference in these structures between control and FUT1$^{-/-}$ mice. Thus, loss of FUT1 appeared to slow the maturation of the nerve fibre and glomerular layers without producing any lasting defect.

We next examined whether loss of FUT1 affected the topographical targeting of primary axons in the main olfactory bulb of early postnatal animals. Immunostaining for the cell adhesion molecule OCAM, which labels a subpopulation of primary olfactory axons terminating in the ventral main olfactory bulb (Alenius and Bohm, 1997; Yoshihara et al., 1997), revealed no difference in distribution of these axons between the FUT1$^{-/-}$ and control mice (arrows, Figs. 1H, I). Another marker of primary olfactory axons is the lectin *Dolichos biflorus* agglutinin (DBA) which recognizes cell surface N-acetyl-galactosamines that are expressed by a subpopulation of axons that terminate in the rostro-dorsal and in the ventral main olfactory bulb (Key and Akeson, 1993) (arrows, Fig. 1J). Again there was no difference in the distribution of these axons between control and FUT1$^{-/-}$ mice (Fig. 1K). Together these results revealed that while loss of the BGH carbohydrate slowed the maturation of the nerve fibre and glomerular layers during the early postnatal period it had no effect on the topographical targeting of axons in the main olfactory bulb.

We were also interested in determining whether loss of FUT1 disrupted the development or topography of axons in the accessory olfactory bulb. Primary sensory axons of the accessory olfactory system arise from the vomeronasal organ (VNO) and terminate in the accessory olfactory bulb. There are two clearly distinct subpopulations of these neurons. Those that terminate in the rostral half of the accessory olfactory bulb express OCAM (Yoshihara et al., 1997, arrowhead Fig. 1H), while those that terminate in the remaining caudal domain express the carbohydrate recognized by the *Bandeiraea simplicifolia* lectin I-B4 (BSI-B4, Salazar and Sanchez Quinteiro, 2003). We have also identified here a new third subpopulation of VNO neurons that expressed the blood group A (BGA) carbohydrate antigen, which is synthesized by addition of a terminal N-acetyl-galactosamine residue to the BGH precursor (Fig. 1C). The BGA positive axons selectively innervated the caudal one third of the accessory olfactory bulb at P2.5 (Figs. 1L, M). However, over the next 3 weeks the expression of BGA increased until all VNO axons expressed this carbohydrate (Figs. 1N, O). Throughout this period BGA was restricted only to the accessory olfactory system; no axons in the main olfactory bulb expressed this carbohydrate.

To determine whether there was any delay in development of the accessory olfactory bulb similar to that observed in the main olfactory bulb, we measured the size of the accessory olfactory bulb and examined the glomerular layer. However, no differences were detected between control and FUT1$^{-/-}$ mice. We next compared the topography of the terminations of VNO axons expressing OCAM, BSI-B4 and BGA in both the FUT1$^{-/-}$ and control mice. We found that loss of FUT1 had no effect on the distribution of OCAM (Figs. 1H, I) and BSI-B4 (Figs. 1Q, R) axons in the accessory olfactory bulb. However, in the absence of FUT1 there was no longer any expression of BGA by the VNO neurons (Figs. 1O, P). This is understandable since the BGH carbohydrate, which is lost in FUT1$^{-/-}$ mice, is the substrate for the BGA glycosyl-transferase (BGAT) which transfers N-acetyl-galactosamine to the BGH substrate (Fig. 1C). Thus, despite the loss of BGA as well as BGH there was no gross effect on the targeting of axons along the rostro-caudal axis of the accessory olfactory bulb. While these results suggest that loss of these carbohydrates does not affect VNO axon targeting it is possible that other molecules such as OCAM and the BSI-B4 carbohydrate have functions that preserve topography in the FUT1$^{-/-}$ mice.

Generation of BGAT gain-of-function transgenic mice

Since loss of BGA from VNO axons did not produce a phenotype in the accessory olfactory system we next adopted a gain-of-function approach in order to further examine its role. We generated transgenic mice which mis-expressed the BGAT under the control of the promoter for the olfactory marker protein (OMP) gene (Danciger et al., 1989) (Fig. 2A). Since BGH is expressed by all sensory neurons (both primary olfactory and VNO neurons), and it is the substrate for BGAT, we postulated that the ubiquitous expression of BGAT would lead to widespread expression of BGA similar to the distribution

of BGH. This strategy proved effective and resulted in the expression of the BGA carbohydrate by sensory axons throughout the olfactory systems from early in development.

The efficacy of BGAT transgene expression was demonstrated by BGA immunostaining of primary olfactory neurons and their axons as early as E12.5 (Fig. 2C). There was no BGA expression in control littermates at this age. At E13.5, numerous primary olfactory neurons and their axons were strongly expressing BGA (Figs. 2D–F). Double labeling of tissue sections for OMP and BGA revealed that BGA was ectopically expressed by many primary olfactory neurons in the olfactory neuroepithelium and their axons in the bulb at this age (Figs. 2G–G″). This staining was near ubiquitous by E15.5 (Figs. 2H–H″) and continued throughout embryogenesis (Figs. 2G′–I′). Most neurons co-expressed OMP and BGA at E17.5 (Figs. 2J–J″). Control littermate mice first showed expression of BGA at P2.5 when a small subpopulation of accessory olfactory axons expressed the carbohydrate (Figs. 1L, M). In contrast, in the transgenic mice BGA was detected as early as E13.5 in the VNO (Fig. 2K) and by P2.5 was present on most OMP positive neurons in the VNO (Figs. 2L–L″). At P2.5, rather than being restricted to a subpopulation of VNO axons as in control mice (Figs. 1L, M), BGA was expressed by all sensory axons and their glomerular terminations in both the main and accessory olfactory bulbs of transgenic animals (Fig. 3A). Moreover, in the BGAT over-expressing animals BGA was present on axons that terminated in both the rostral and caudal regions of the accessory olfactory bulb, even during the early postnatal period when BGA is normally restricted to only the caudal one third of this structure in wild type mice (Figs. 1L, M).

Four stable founder lines of transgenic mice (BGAT-Tg) were generated and all mice that genotyped as BGAT-Tg positive also exhibited BGA immunostaining on sensory axons throughout the main olfactory and accessory olfactory bulbs, indicating full penetrance of the blood group A glycosyltransferase transgene. All lines displayed similar expression of BGA carbohydrate and two lines (BGAT-Tg 102 and BGAT-Tg 2/4) were subsequently maintained and analysed. These lines had denser BGA immunostaining in the main olfactory bulb compared to the accessory olfactory bulb (Fig. 2B) and since they exhibited identical phenotypes we will refer to them as BGAT-Tg. Taken together, the expression data indicate that we were able to achieve our goal of mis-expressing BGA in the olfactory system from the very earliest stages of development when axons are actively establishing the olfactory nerve pathway as well as during the neonatal period when glomeruli are being refined (Key and St John, 2002).

Ectopic expression of BGA causes exuberant axon growth in the accessory olfactory bulb

The most obvious and striking phenotype in the BGAT-Tg mice was the presence of over-projecting axons in the deeper lamina of the accessory olfactory bulb (Figs. 3A, B). The immunostaining for BGA clearly revealed that some sensory axons displayed exuberant growth and projected past their normal targets in the glomerular layer and coursed extensively and inappropriately within the underlying external plexiform layer. No such growth was detected in wild type animals (Figs. 1L, M). Interestingly, there was no difference between control and BGAT-Tg mice in the extent of overgrowth in the main olfactory bulb. While there is a basal level of exuberant growth by primary olfactory neurons during the early postnatal period in the main olfactory bulb (St John and Key, 2005; Tenne-Brown and Key, 1999), this was unaffected by the ectopic expression of BGA in these neurons (data not shown).

In order to determine the origin of the over-projecting axons in the accessory olfactory bulb we impregnated the VNO with the neuroanatomical tracer DiI. This dye clearly labelled the VNO nerve and its terminations in the accessory olfactory bulb in P2.5 animals (Figs. 3D, E). Using this approach, DiI labeled axons were never observed to over-project past the glomerular layer in control animals (Fig. 3F; $n=7$). In contrast, in all BGAT-Tg littermates ($n=5$) axons were observed inappropriately projecting past the target glomerular layer and into deeper layers in the accessory olfactory bulb (Figs. 3G, H), as we had observed using BGA immunostaining (Fig. 2B). Over-projecting axons in BGAT-Tg mice displayed various trajectories and were observed either individually (arrowhead, Fig. 3G) or in small fascicles (arrowhead, Fig. 3H) in the external plexiform layer. Many of these axons appeared to loop and project back towards the glomerular layer (arrows, Figs. 3G, H). These results confirmed our observations obtained by immunohistochemical staining (Fig. 3B) and revealed that these axons were growing from the VNO and were not misguided sensory axons from the main olfactory bulb.

In wild type mice at P21, BGA was present uniformly throughout the nerve fibre and glomerular layers of both the rostral and caudal halves of the accessory olfactory bulb (Figs. 1O, 4A), at expression levels which were comparable to that observed in the BGAT-Tg mice of similar age (Fig. 4B). It was now possible to observe occasional short over-projecting axons in the deeper layers of the accessory olfactory bulb in wild type mice (Fig. 4C). In contrast, all BGAT-Tg mice had numerous fascicles of axons in the external plexiform layer of the accessory olfactory bulb at this age (Figs. 4B, D, E). We counted the number of axons present in the external plexiform layers of control and BGAT-Tg mice and found that BGAT-Tg mice had 2.7 times more axons ($n=8$, $p<0.005$, SEM 0.4). However, this quantification is likely an underestimate of the actual number of axons since most axons in the BGAT-Tg were in small fascicles (Fig. 4E) making it necessary to instead count fascicles, whereas axons in control mice appeared to be isolated single axons. Interestingly, this exuberant growth phenotype was not observed in the FUT1$^{-/-}$ mice. Thus, BGA gain-of-function rather than loss-of-function produced this aberrant growth.

The overgrowth of axons in the BGAT-Tg could possibly arise because mis-expression of BGAT may have altered the expression of other blood group carbohydrates in the accessory olfactory bulb. To test this we examined the expression of BGH and blood group B and found no difference between control and BGAT-Tg mice in the distribution of these

carbohydrates in the accessory olfactory bulb (Figs. 4F–I). We also examined the expression of other carbohydrates in the accessory olfactory bulb using lectins (LEA, PA, and SBA) and anti-carbohydrate monoclonal antibodies (Mab LA4, Mab 9OE and Mab KH10) previously shown to be expressed in the olfactory system (Key and Akeson, 1990; Key and Giorgi, 1986; Salazar et al., 2001; Storan et al., 2004). In all cases, the various carbohydrates recognized by these probes showed identical expression patterns in both control and BGAT-Tg littermates (data not shown). Thus mis-expression of BGAT

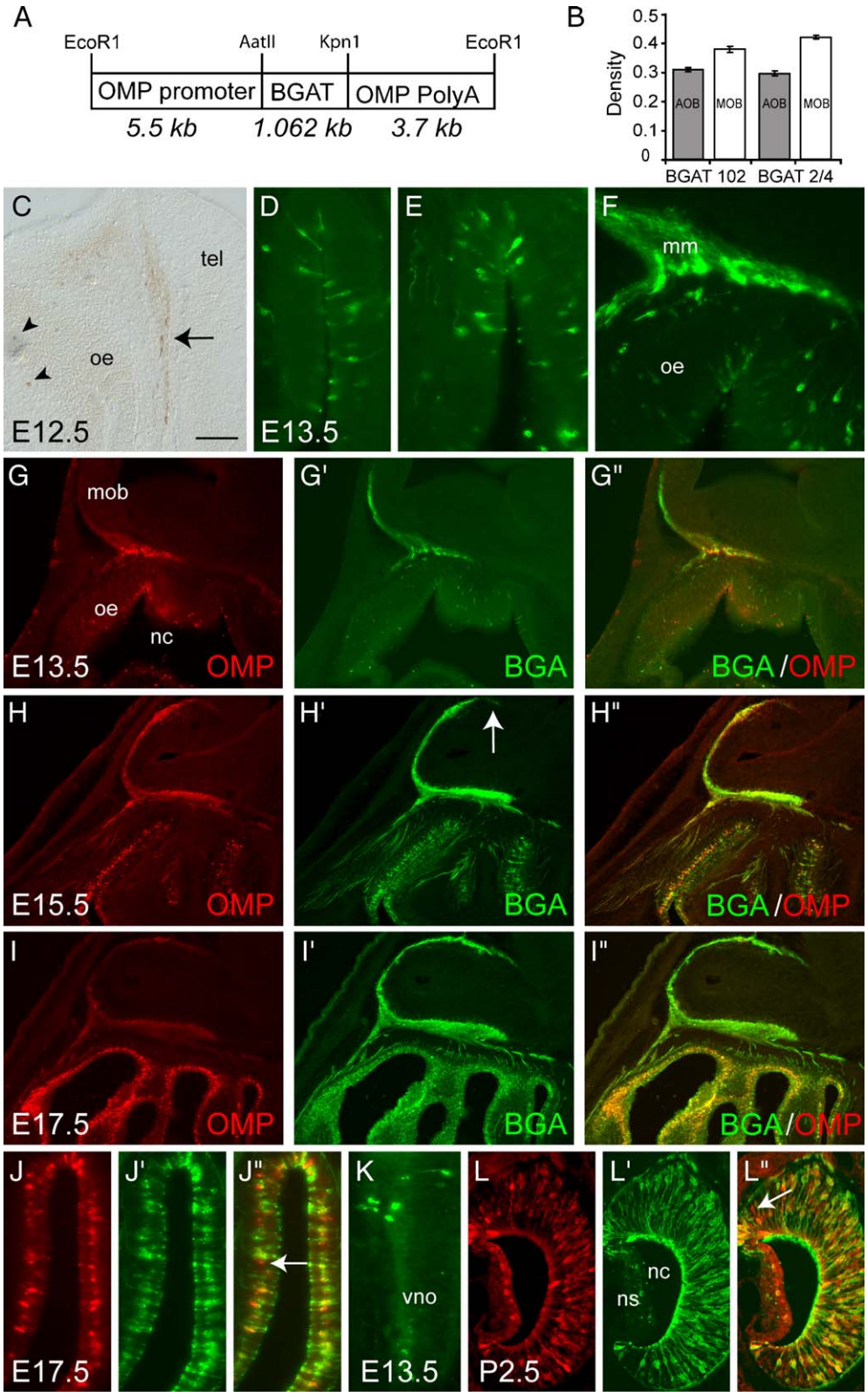

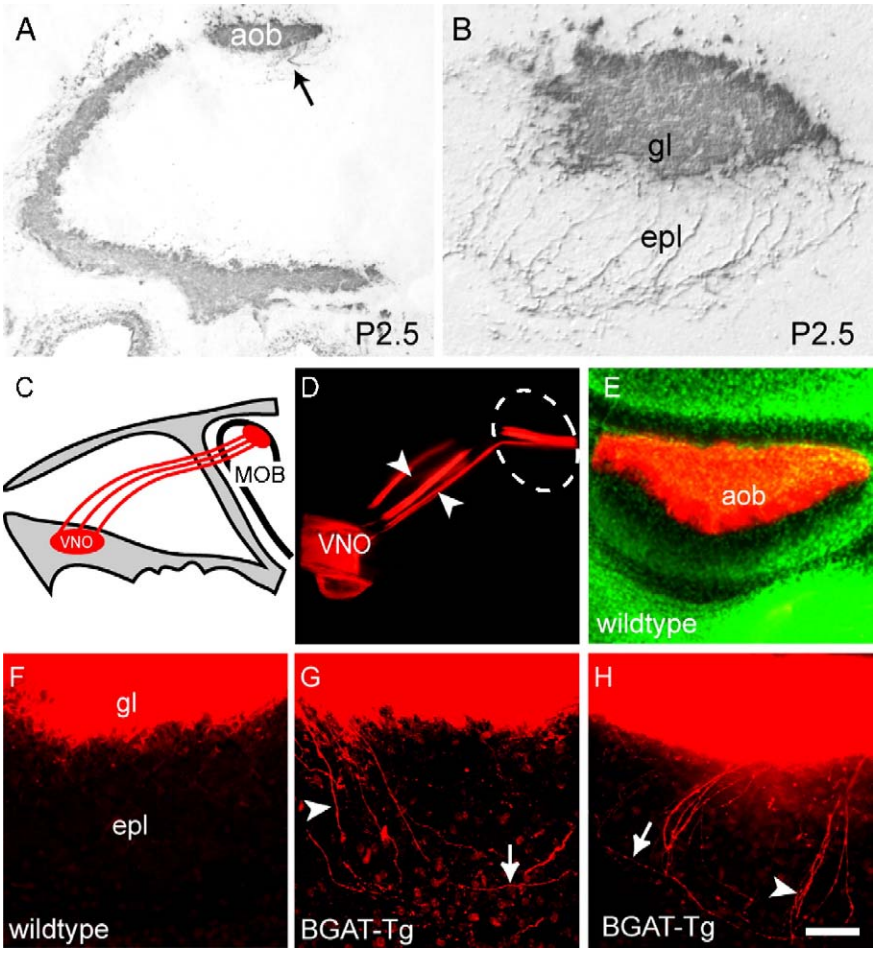

Fig. 3. VNO axons over-project in BGAT transgenic mice. (A) In P2.5 BGAT-Tg mice, BGA was strongly expressed by primary axons in both the main and accessory olfactory bulbs. Numerous axons over-project in the AOB (arrow). (B) Higher power view of BGA immunostaining in the AOB of BGAT-Tg mice showing numerous axons over-projecting past the glomerular layer (gl) into deeper inappropriate layers. (C) Schematic showing the vomeronasal (VNO) axons projecting to the AOB which is dorsal and caudal to the main olfactory bulb (MOB). (D) DiI that was injected into the VNO of P2.5 wild type and BGAT-Tg littermates was transported along the axons to the accessory olfactory bulb; dotted circle shows location of main olfactory bulb. (E) After 2 months, DiI was present throughout the accessory olfactory bulb of wild type and BGAT-Tg mice (wild type shown); section is counter-stained with acridine orange (green). (F) In wild type mice, DiI labelled axons terminated in the glomerular layer (gl), but were not observed within the epl. (G) In BGAT-Tg mice, axons over-projected past the glomerular layer into the external plexiform layer. Single axons were observed (arrowhead) and often looped back (arrow). (H) Axons were also observed in small fascicles (arrowhead) and looped back (arrow). nc, nasal cavity; ns, non-sensory epithelium; tel, telencephalon. Scale bar is 120 μm in panel A; 60 μm in panels B, E; 640 μm in panel D; 30 μm in panels F–H.

did not affect the overall composition of cell surface carbohydrates on VNO axons. These results suggest that the altered expression of BGA was directly responsible for the exuberant overgrowth of VNO axons rather than being a secondary effect of altered expression of other carbohydrates in the accessory olfactory bulb.

Fig. 2. Blood Group A carbohydrate is ectopically expressed in BGAT transgenic mice. (A) The 1.05 kb coding sequence for human histo-blood group A glycosyltransferase (BGAT) is under the control of the 5.5 kb OMP promoter. (B) Comparison of BGA immunostaining density between two founder lines of BGAT-Tg mice at P2.5. In the accessory olfactory bulb (shaded columns) immunostaining density in the two lines was the same ($p > 0.05$). In the main olfactory bulb (open columns) the BGAT 2/4 line had denser staining than the BGAT 102 line ($p < 0.05$). Panels C–I are parasagittal sections with rostral to the left and dorsal to the top. (C) In transgenic BGAT-Tg mice, BGA was first expressed at E12.5 in the olfactory neuroepithelium (oe) (arrowheads) and migratory mass (arrow). OMP immunostaining is red, BGA immunostaining is green in panels D–L. (D–F) In E13.5 BGAT-Tg mice, BGA was strongly expressed by primary olfactory neurons in the main olfactory neuroepithelium. (G) OMP immunostaining is first expressed in E13.5 BGAT-Tg mice. (G′) In these mice, BGA was strongly expressed by primary olfactory axons in the migratory mass lining the rostral surface of the presumptive main olfactory bulb (mob). (G′, G″) Interestingly, at this age fluorescence staining for ectopic BGA was stronger than that observed for endogenous OMP. In E15.5 (H) and E17.5 (I) BGAT-Tg animals, BGA was expressed by axons in the main and accessory (arrow) olfactory bulbs. Again the immunostaining for BGA was stronger than for OMP (H′, H″; I′, I″). (J) In the main olfactory neuroepithelium of E17.5 BGAT-Tg mice, the vast majority of neurons expressed both OMP (J) and BGA (J′); however, a small number of neurons expressed OMP but not BGA (arrow in panel J″). (K) A parasagittal section of the vomeronasal organ in a BGAT-Tg embryo at E13.5. BGA was first expressed in the vomeronasal organ at this age. (L) In the vomeronasal organ, the vast majority of primary accessory olfactory neurons expressed both OMP (L) and BGA (L′), although a few neurons (arrows) expressed OMP, but not BGA (arrow in L″). nc, nasal cavity; ns, non-sensory epithelium; tel, telencephalon. Scale bar is 160 μm in panel C; 100 μm in panels G–I; 40 μm in panels D–F; 20 μm in panels J, K; 60 μm in panel L.

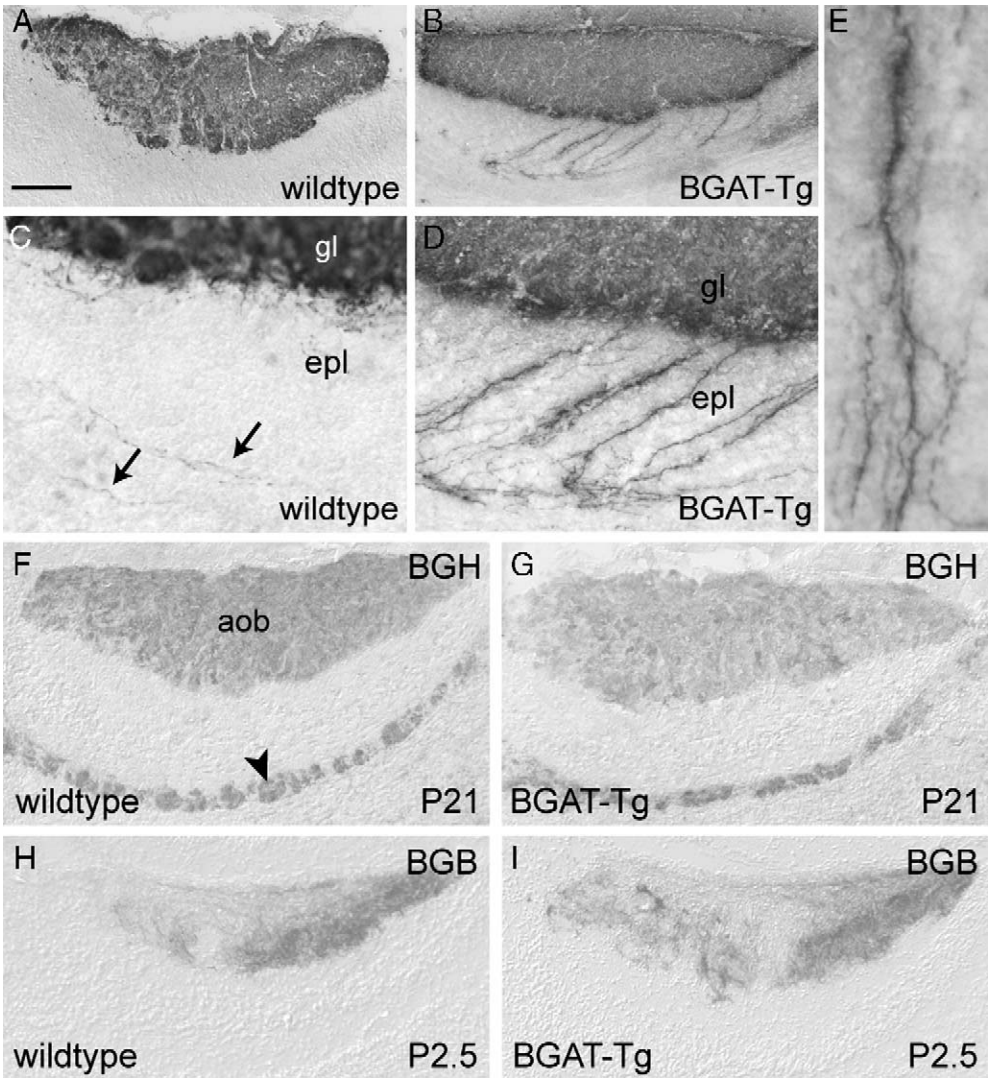

Fig. 4. Axons over-project past the glomerular layer in the AOB. (A) In P21 wild type mice, BGA is uniformly and strongly expressed throughout the AOB. (B) In BGAT-Tg mice, numerous over-projecting axons are obvious. (C) In P21 wild type mice, axons (arrows) immunostained by antibodies against BGA are occasionally observed in the external plexiform layer (epl) of the accessory olfactory bulb. (D) In P21 BGAT-Tg mice, numerous axons that over-projected past the glomerular layer (gl) are present in the external plexiform layer. (E) Higher power image of over-projecting axons in a BGAT-Tg mouse. Often axons formed small fascicles; due to the difficulty in identifying individual axons, fascicles were counted. (F) In P21 wild type mice, BGH is strongly expressed throughout the AOB as well as by second order axons in the lateral olfactory tract (arrowhead). (G) In P21 BGAT-Tg mice, BGH continues to be expressed throughout the AOB. (H) BGB is widely expressed in glomeruli in the caudal AOB as well as some glomeruli in the rostral AOB of P2.5 wild type mice. (I) In BGAT-Tg mice, BGB expression maintains its restricted distribution. Rostral is to the left and dorsal to the top in panels A–D, F–I. Scale bar is 230 μm in panels A, B; 50 μm in panels C, D, 30 μm in panel E; 100 μm in panels F, G; 80 μm in panels H, I.

The topography of VNO axons is unaffected by ectopic expression of BGA

Since BGA mis-expression led to an overgrowth of VNO axons in the accessory olfactory bulb we were interested in determining whether there were also defects in the topography of this pathway. Histochemical staining with the lectin BSI-B4 revealed that the axons that normally terminated in the caudal half of the accessory olfactory bulb continued to project appropriately in the BGAT-Tg mice (Fig. 5B) as in controls (Fig. 5A). It should be noted that BSI-B4 diffusely stains the caudal half of the accessory olfactory bulb without clear resolution of individual axons. To more clearly examine the topography of this pathway we crossed the BGAT-Tg mice with the previously generated V1rb2-GFP (Rodriguez et al., 1999) and V2r1b-GFP lines of mice (Del Punta et al., 2002). In these animals, the green fluorescence protein GFP was selectively expressed by only those VNO neurons expressing either the V1rb2 or the V2r1b receptor. V1rb2 axons target glomeruli which are typically aligned along the rostral side of the midline border between the rostral and the caudal halves of the accessory olfactory bulb (Fig. 5C). Several additional labelled glomeruli are also located towards the rostral tip of the accessory olfactory bulb (arrows, Fig. 5C). In contrast, V2r1b axons project to glomeruli located along the caudal side of the midline border in the accessory olfactory bulb (Fig. 5E). In the BGAT-Tg mice crossed with these reporter lines we found no difference in the topography

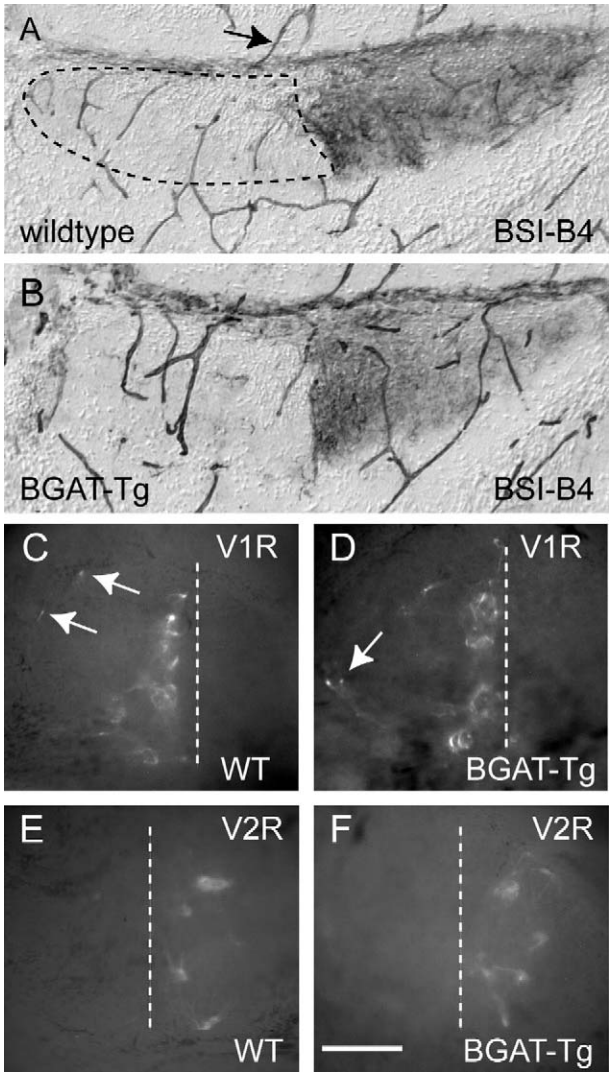

Fig. 5. Glomerular targeting is maintained. (A) In P2.5 wild type mice, the lectin BSI-B4 labels axons that terminate in the caudal AOB. Blood vessels that express the carbohydrate recognised by the lectin are also stained (arrow). (B) BSI-B4 staining continues to delineate the rostro-caudal division of the AOB in BGAT-Tg mice. In wholemount views of the AOB in 2-week-old V1rb2-GFP mice crossed with BGAT-Tg mice, the position and number of V1R glomeruli is similar between mice BGAT-Tg mice (D) and wild type mice (C). When V2r1b-GFP mice were crossed with BGAT-Tg mice, there was no difference in the position or number of V2R glomeruli in BGAT-Tg mice (F) compared to wild type mice (E). Panels A, B are parasagittal; rostral is to the left. Panels C–F are wholemount views with rostral to the left and medial to the bottom. Scale bar is 80 μm in panels A, B; 100 μm in panels C–F.

of the glomeruli within either the rostral or caudal halves of the accessory olfactory bulb (Figs. 5D, F). Taken together, these results confirmed our observations from the BSI-B4 staining indicating that ectopic expression of BGA does not change the topography of the VNO nerve pathway. We also examined whether over-projecting axons of the V1R and V2R subpopulations were present in parasagittal sections of BGAT-Tg mice crossed with the reporter lines. However, we did not detect any of these axons projecting inappropriately into the deeper layers. This result raises the possibility that mis-expression of BGA selectively affected subpopulations of axons other than those expressing V1R and V2R.

Mis-expression of BGA in the main olfactory bulb causes aberrant growth of primary olfactory axons in the glomerular layer

Although ectopic expression of BGA had no effect on the extent of over-projecting axons in the main olfactory bulb we next examined whether the pathfinding of axons in the main olfactory bulb was normal in the BGAT-Tg animals. Staining for OCAM and the DBA ligand revealed that there was no gross defect in the topography of the main olfactory nerve pathway (not shown), which was consistent with the absence of similar defects in the FUT1$^{-/-}$ mice (see Figs. 1H–K). We next crossed the BGAT-Tg mice with the M72-IRES-tau:GFP line of mice (Potter et al., 2001) which expresses GFP only in primary olfactory neurons expressing the M72 odorant receptor. At 3 weeks of age the M72 axons converge on two glomeruli in the dorso-caudal olfactory bulb (Potter et al., 2001). Since the compact and flattened morphology of the dorso-lateral glomerulus made analysis of axon pathfinding to this topographical position difficult we concentrated our analysis on the M72 glomerulus on the medio-dorsal surface. In P21 control mice, the majority of M72-GFP axons projected to the target glomerulus in 1–2 large fascicles (arrow, Fig. 6A). In addition, a small number of separate individual axons projected aberrantly in the glomerular layer (arrowheads, Fig. 6A; Figs. 6B–G). In BGAT-Tg mice the number of aberrantly projecting axons in the glomerular layer (Figs. 6H–N) was 4.2 times higher than in wild type mice ($p<0.01$, $n=10$; SEM=1.2). These mis-routed axons typically projected either around or into glomeruli surrounding the M72 glomerulus (Figs. 6J–N). Not only were there significantly more axons but the combined total length of individually projecting axons in the glomerular layer of BGAT-Tg mice was 3.7 times greater than that detected in wild type animals ($p<0.01$, $n=10$; SEM=1.2).

We next analysed the distribution of these mis-routed axons. In the coronal plane, most of the mis-routed axons in BGAT-Tg mice projected dorsal to the M72 glomerulus (Figs. 6H, I). Occasionally, however, some axons were up to 500 μm ventral to the M72 glomerulus (Figs. 6H, I). The average maximum dorso-ventral distribution of the mis-routed axons in BGAT-Tg animals was 1.9 times larger than in wild type mice ($p<0.05$; $n=10$; SEM=0.4). Along the rostro-caudal axis in BGAT-Tg animals, the mis-routed M72-GFP axons were distributed over a 1.4 times larger distance compared to wild type mice ($p<0.05$; $n=10$; SEM=0.2). Thus, while the main olfactory bulb of BGAT-Tg mice did not exhibit any increase in the over-projection of axons into the deeper lamina as in the accessory olfactory bulb there were significant pathfinding errors within the glomerular layer.

Discussion

The restricted expression of specific glycans by subpopulations of primary sensory neurons in the main and accessory

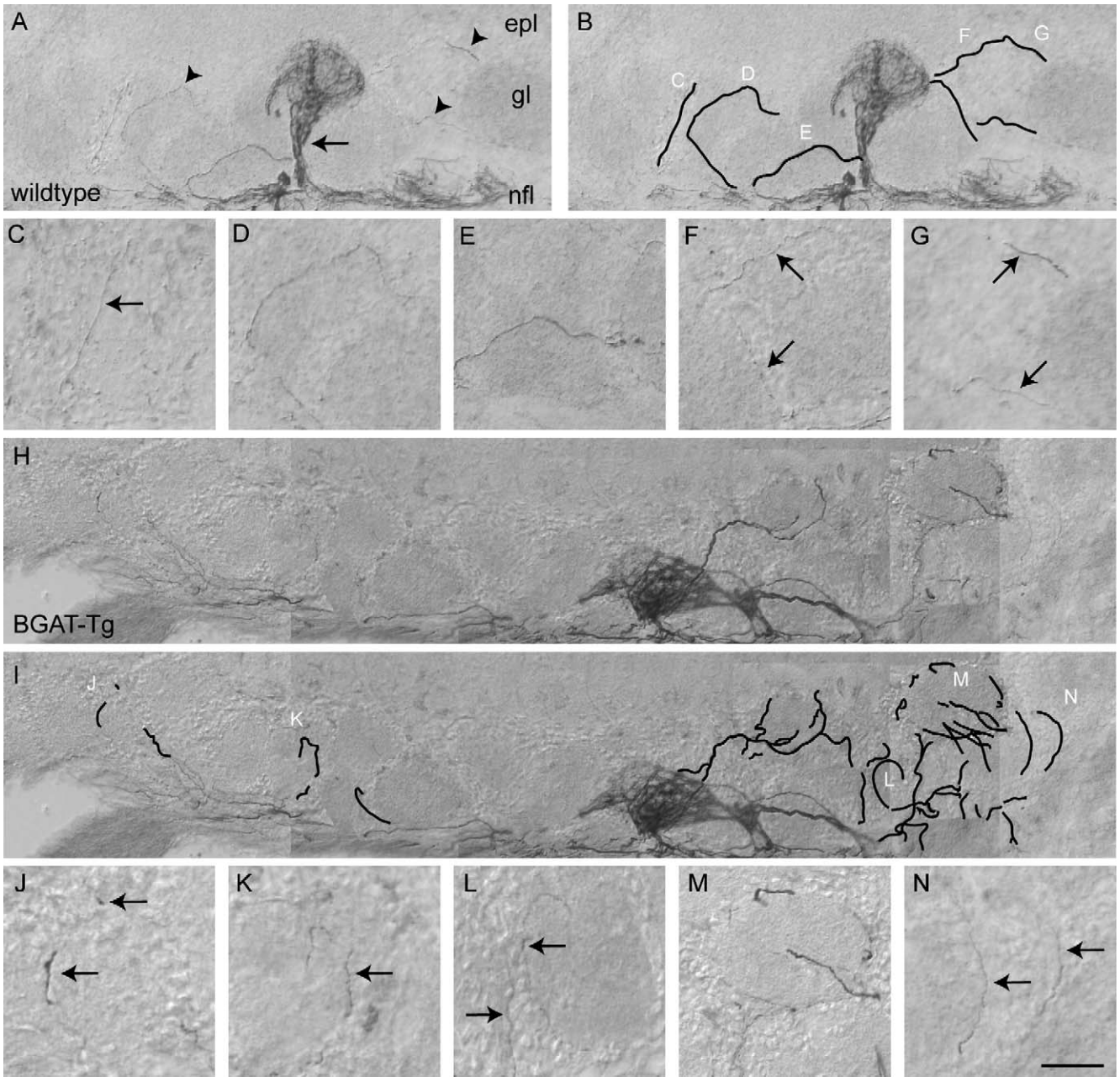

Fig. 6. Targeting of M72 axons is perturbed in BGAT-Tg mice. Panels A and G are montages of photographs of serial coronal sections of M72-GFP axons targeting the medial surface of the olfactory bulb immunostained with anti-GFP. As overlaying the photographs obscured the views of axons in the different layers, the projections of all axons were traced in Adobe Illustrator by sequentially adding in irregular shaped layers and are shown in panels B and I. (A and B) In 3-week-old wild type mice, axons that were present in the glomerular layer were typically en route to the M72 glomerulus. (C–G) Higher power images of the axons labelled in panel B. (H and I) In BGAT-Tg littermates, numerous M72-GFP axons were present in the glomerular layer neighbouring the M72 glomerulus and individual axons were observed up to 500 μm ventral to the M72 glomerulus. (J–N) Higher power images of the axons labelled in I. Panels A–N are coronal; ventral is to the left, medial is to the bottom. Epl, external plexiform layer; gl, glomerular layer; nfl, nerve fibre layer. Scale bar is 50 μm in panels A, B, H, I; 20 μm in panels C, I, M, N; 25 μm in panels E, J, K; 30 μm in panels D, F, L.

olfactory systems has led us to previously propose the hypothesis that the selective expression of cell surface carbohydrates by sensory axons is pivotal for the normal development of the olfactory nerve pathway (Key and St John, 2002). We showed here that the blood group A (BGA) carbohydrate is selectively expressed by a subpopulation of vomeronasal organ (VNO) neurons which terminate in a subregion of the caudal half of the neonatal mouse accessory olfactory bulb. BGA was absent in the main olfactory bulb. This selective expression pattern of BGA provided an opportunity to test the above hypothesis by examining loss-of-function mice lacking the α(1,2)fucosyltransferase FUT1 and a novel transgenic gain-of-function line of mice that mis-expresses the blood group A glycosyltransferase (BGAT) selectively in the olfactory system. FUT1 is responsible for the synthesis of the blood group H (BGH) carbohydrate antigen by both VNO and olfactory

primary sensory neurons. Because the BGH carbohydrate is the substrate for BGAT, the BGA carbohydrate was also missing from VNO neurons in the FUT1$^{-/-}$ mice.

Loss of BGH from all primary sensory axons in the developing main olfactory system in the FUT1$^{-/-}$ mice resulted in delayed development of the nerve fibre and glomerular layers of the main olfactory bulb. In particular, during the neonatal period there were fewer large glomeruli and the nerve fibre layer was thinner in the FUT1 deficient mice. We have previously observed similar defects in the olfactory bulb of NCAM-180 knockout mice which also lack the poly-α(2,8)sialic acid carbohydrate (Treloar et al., 1997). The polysialic acid glycan plays an important role in regulating the function of NCAM in vivo (Weinhold et al., 2005). However, BGH present on NCAM may play a more direct role in neuronal morphology and synaptogenesis. The fucose-α(1,2)galactose residue that forms the BGH glycan has recently been shown to specifically enhance neurite outgrowth and synapse formation in vitro (Kalovidouris et al., 2005; Murrey et al., 2006). The idea that fucosylated glycoproteins are involved in synaptic plasticity is not new, since earlier studies in chicks and mice had shown that enhanced memory formation involved increased fucosylation (Lorenzini et al., 1997; Mileusnic et al., 1995). Thus, the defects we observed in the olfactory system could easily arise because of the role of fucose-α(1,2)galactose in axon growth and synaptogenesis. Fucosylated glycoproteins are, however, not alone in their ability to modulate neuronal morphology since other synapse specific glycans are also important in synaptic interactions (Martin et al., 1999; Parkhomovskiy et al., 2000; Xia et al., 2002). Thus, these and other molecules may have redundant functions that explain why the retarded growth in the olfactory system was only transient. By 3 weeks postnatally, the morphology of the outer layers of the bulb appeared normal in the FUT1$^{-/-}$ mice.

The recovery of the nerve fibre and glomerular layer development in the FUT1$^{-/-}$ mice is not surprising. In β1,3-*N*-acetylglucosaminyltransferase knockout mice, there was an initial loss of a number of lactosamine carbohydrates which resulted in widespread death of primary olfactory neurons and subsequent poor innervation of the olfactory bulb during development (Henion et al., 2005). Interestingly, these carbohydrates were re-expressed in the adult via unknown redundant pathways and appropriate targeting was restored. In the zebrafish, loss of heparan sulphate proteoglycans in *Ext* mutants perturbs the ability of axons to topographically sort out within the optic tract causing the axons to enter the tectum via an inappropriate branch of the tract. However, despite this perturbed sorting the axons still managed to reach their appropriate target (Lee et al., 2004). Again this indicates that while specific glycans contribute to axon growth, guidance or fasciculation it is clear other guidance cues are involved and perturbed expression of carbohydrates can be compensated by other molecules. Moreover, transient phenotypes are not uncommon, especially in highly redundant pathways. In mice lacking Robo 1 there was a mild transient phenotype in midline crossing at E11.5 but this error was corrected by E12.5 (Long et al., 2004). In comparison, prominent midline phenotypes were not observed until all three Slits were knocked out (Long et al., 2004) or until the pre-crossing inhibition of Robos to the Slits was abolished (Sabatier et al., 2004).

In the face of the redundancy in the olfactory system we adopted a gain-of-function strategy to disturb glycan expression in the olfactory system. The BGA sugar was forcibly mis-expressed by all primary sensory neurons throughout the main and accessory olfactory system by creating transgenic mice driving expression of BGAT under the control of the OMP promoter. This mis-expression of BGA resulted in the aberrant over-projection of VNO axons in the accessory olfactory bulb as well as increased mis-routing errors within the glomerular layer of the main olfactory bulb. One of the strengths of our approach was that the H-blood group is selectively expressed on NCAM and that over-expression of BGA was restricted to this molecule. Thus, the chances of global non-specific defects occurring were reduced and in fact, this was proven by the absence of severe mutant phenotypes. What we have achieved here is a selective manipulation of carbohydrate expression in the BGAT-Tg mice that results in neuron survival and robust innervation of the olfactory bulb. Both the Fut1$^{-/-}$ and BGAT-Tg mutant mice displayed axon trajectory defects which were consistent with cell surface carbohydrates contributing to axon guidance.

BGH and BGA carbohydrates have both been implicated in axon growth or guidance in other systems. We have previously shown that BGA plays a role in axon–axon recognition in the Xenopus embryonic brain (Anderson and Key, 1999); and others have shown that BGH stimulates neurite outgrowth of hippocampal neurons in vitro (Kalovidouris et al., 2005). Other fucosylated carbohydrates can also modulate axon growth. The fucosylated Lewis-X blood group carbohydrate is expressed by neurons in the optic chiasm in mice and exogenously applied Lewis-X inhibits retinal neurite outgrowth in vitro (Lin et al., 2005). Antibody blocking of Lewis-X also prevents neurite outgrowth from explants of Xenopus brain (Yoshida-Noro et al., 1999). Within the olfactory system, inhibiting the binding of lactosamine carbohydrates in rat olfactory neuroepithelial explants reduces axon fasciculation, but does not affect axon outgrowth (Storan et al., 2004). Thus, the response of axons to carbohydrate interactions is varied and cell-context specific.

In the loss-of-function FUT1$^{-/-}$ mice, the delay in the development of the nerve fibre and glomerular layer was recovered in the adult. In the gain-of-function BGAT-Tg mice it was apparent that while a subpopulation of axons overshot their termination zone in the accessory olfactory bulb or mis-routed in the main olfactory bulb, the majority of axons successfully navigated to their appropriate target. Thus, in both models axons were either able to eventually target correctly or the majority of axons were initially successful despite the perturbed carbohydrate expression. These results are consistent with the considerable degree of redundancy in the genetic control of axon growth in the olfactory system. In mice lacking Neuropilin-2, a small subset of main olfactory axons overshoot the glomerular layer whereas some accessory

olfactory axons fail to fasciculate correctly and hence terminate in abnormal targets (Cloutier et al., 2002; Walz et al., 2002). Similarly, in mice lacking Sema3F, which is the Neuropilin-2 ligand, some accessory olfactory axons do not fasciculate properly and some main olfactory axons overshoot the glomerular layer (Cloutier et al., 2004). Similarly, loss of Close homolog of L1 (Montag-Sallaz et al., 2002), olfactory cyclic nucleotide-gated channel subunit (OCNC1, Zheng et al., 2000) or Olfactory Marker Protein (OMP, St John and Key, 2005) also increases the extent of over-projecting of olfactory sensory axons in the olfactory bulb. In all cases the phenotypes were only partially penetrant which suggest that complex multi-gene interactions are controlling axon growth and guidance in the olfactory system. It is also interesting that in these various mutant mice that the VNO axons and primary olfactory axons typically responded differently to these perturbations, just as we observed in the FUT1$^{-/-}$ and BGAT-Tg mice.

While the molecular mechanism by which these cell surface carbohydrates regulate axon growth in the olfactory system remains uncertain, it is clear that these molecules can act as direct ligands for carbohydrate binding proteins such as galectins which are active in the olfactory system (Crandall et al., 2000; Puche et al., 1997), and that they can modulate the activity of adhesion molecules such as NCAM (Weinhold et al., 2005) or of synaptic molecules (Martin et al., 1999, 2002; Murrey et al., 2006; Parkhomovskiy et al., 2000). Why should BGA produce a phenotype in the main olfactory system where it is not normally expressed? Clearly this gain-of-function phenotype could arise by either modulating the activity of NCAM directly or through cis and trans interactions with guidance/growth receptors common to both pathways. Interestingly, the mis-expression of BGAT produced exuberant growth of sensory axons in both the main and olfactory systems which supports conservation of function of this molecule in these different pathways. The results of the BGAT-Tg and FUT1$^{-/-}$ mice demonstrate that cell surface carbohydrates contribute to axon guidance in the olfactory system and add support to the hierarchical model of olfactory axon guidance (Key and St John, 2002). In this model the ability of olfactory axons to target topographically-fixed glomeruli is dependent on the coordinated expression of various guidance cues acting throughout the olfactory nerve pathway. Distinct molecules mediate different cellular responses and behaviors that facilitate the initial fasciculation, and then the selective defasciculation, sorting and refasciculation in the nerve fibre layer of the main olfactory and accessory olfactory bulbs prior to glomerular formation. We have shown here that the guidance of sensory axons is mediated in part by cell surface carbohydrates.

Acknowledgments

This work was supported by grants from the National Health and Medical Research Council to J.St.J and B.K. We thank Dr. F. Margolis for generously providing the clone of the OMP promoter. Ms Katie Lineburg, Ms Linh Nguyen and Ms Tracey Ainsworth provided excellent technical assistance and Ms Victoria Hunter provided valuable assistance with the maintenance of the mouse colony.

References

Alenius, M., Bohm, S., 1997. Identification of a novel neural cell adhesion molecule-related gene with a potential role in selective axonal projection. J. Biol. Chem. 272, 26083–26086.

Allen, W.K., Akeson, R., 1985. Identification of a cell surface glycoprotein family of olfactory receptor neurons with a monoclonal antibody. J. Neurosci. 5, 284–296.

Anderson, R.B., Key, B., 1999. Novel guidance cues during neuronal pathfinding in the early scaffold of axon tracts in the rostral brain. Development 126, 1859–1868.

Aoki, K., Nakahara, Y., Yamada, S., Eto, K., 1999. Role of polysialic acid on outgrowth of rat olfactory receptor neurons. Mech. Dev. 85, 103–110.

Astic, L., Le Pendu, J., Mollicone, R., Saucier, D., Oriol, R., 1989. Cellular expression of H and B antigens in the rat olfactory system during development. J. Comp. Neurol. 289, 386–394.

Cloutier, J.F., Giger, R.J., Koentges, G., Dulac, C., Kolodkin, A.L., Ginty, D.D., 2002. Neuropilin-2 mediates axonal fasciculation, zonal segregation, but not axonal convergence, of primary accessory olfactory neurons. Neuron 33, 877–892.

Cloutier, J.F., Sahay, A., Chang, E.C., Tessier-Lavigne, M., Dulac, C., Kolodkin, A.L., Ginty, D.D., 2004. Differential requirements for semaphorin 3F and Slit-1 in axonal targeting, fasciculation, and segregation of olfactory sensory neuron projections. J. Neurosci. 24, 9087–9096.

Crandall, J.E., Dibble, C., Butler, D., Pays, L., Ahmad, N., Kostek, C., Puschel, A.W., Schwarting, G.A., 2000. Patterning of olfactory sensory connections is mediated by extracellular matrix proteins in the nerve layer of the olfactory bulb. J. Neurobiol. 45, 195–206.

Cutforth, T., Moring, L., Mendelsohn, M., Nemes, A., Shah, N.M., Kim, M.M., Frisen, J., Axel, R., 2003. Axonal ephrin-As and odorant receptors: coordinate determination of the olfactory sensory map. Cell 114, 311–322.

Danciger, E., Mettling, C., Vidal, M., Morris, R., Margolis, F., 1989. Olfactory marker protein gene: its structure and olfactory neuron-specific expression in transgenic mice. Proc. Natl. Acad. Sci. U. S. A. 86, 8565–8569.

Del Punta, K., Puche, A., Adams, N.C., Rodriguez, I., Mombaerts, P., 2002. A divergent pattern of sensory axonal projections is rendered convergent by second-order neurons in the accessory olfactory bulb. Neuron 35, 1057–1066.

Domino, S.E., Hiraiwa, N., Lowe, J.B., 1997. Molecular cloning, chromosomal assignment and tissue-specific expression of a murine alpha(1,2)fucosyltransferase expressed in thymic and epididymal epithelial cells. Biochem. J. 327 (Pt. 1), 105–115.

Domino, S.E., Zhang, L., Gillespie, P.J., Saunders, T.L., Lowe, J.B., 2001a. Deficiency of reproductive tract alpha(1,2)fucosylated glycans and normal fertility in mice with targeted deletions of the FUT1 or FUT2 alpha(1,2) fucosyltransferase locus. Mol. Cell. Biol. 21, 8336–8345.

Domino, S.E., Zhang, L., Lowe, J.B., 2001b. Molecular cloning, genomic mapping, and expression of two secretor blood group alpha (1,2) fucosyltransferase genes differentially regulated in mouse uterine epithelium and gastrointestinal tract. J. Biol. Chem. 276, 23748–23756.

Dowsing, B., Puche, A., Hearn, C., Key, B., 1997. Presence of novel N-CAM glycoforms in the rat olfactory system. J. Neurobiol. 32, 659–670.

Ducray, A., Propper, A., Kastner, A., 1999. Detection of alpha-L fucose containing carbohydrates in mouse immature olfactory neurons. Neurosci. Lett. 274, 17–20.

Fujita, S.C., Mori, K., Imamura, K., Obata, K., 1985. Subclasses of olfactory receptor cells and their segregated central projections demonstrated by a monoclonal antibody. Brain Res. 326, 192–196.

Gussing, F., Bohm, S., 2004. NQO1 activity in the main and the accessory olfactory systems correlates with the zonal topography of projection maps. Eur. J. Neurosci. 19, 2511–2518.

Henion, T.R., Raitcheva, D., Grosholz, R., Biellmann, F., Skarnes, W.C., Hennet, T., Schwarting, G.A., 2005. Beta1,3-N-acetylglucosaminyltransferase 1 glycosylation is required for axon pathfinding by olfactory sensory neurons. J. Neurosci. 25, 1894–1903.

Kalovidouris, S.A., Gama, C.I., Lee, L.W., Hsieh-Wilson, L.C., 2005. A role for fucose alpha(1–2) galactose carbohydrates in neuronal growth. J. Am. Chem. Soc. 127, 1340–1341.

Keller, A., Margolis, F.L., 1975. Immunological studies of the rat olfactory marker protein. J. Neurochem. 24, 1101–1106.

Key, B., Akeson, R.A., 1990. Olfactory neurons express a unique glycosylated form of the neural cell adhesion molecule (N-CAM). J. Cell Biol. 110, 1729–1743.

Key, B., Akeson, R.A., 1993. Distinct subsets of sensory olfactory neurons in mouse: possible role in the formation of the mosaic olfactory projection. J. Comp. Neurol. 335, 355–368.

Key, B., Giorgi, P.P., 1986. Soybean agglutinin binding to the olfactory systems of the rat and mouse. Neurosci. Lett. 69, 131–136.

Key, B., St John, J., 2002. Axon navigation in the mammalian primary olfactory pathway: where to next? Chem. Senses 27, 245–260.

Lee, J.S., von der Hardt, S., Rusch, M.A., Stringer, S.E., Stickney, H.L., Talbot, W.S., Geisler, R., Nusslein-Volhard, C., Selleck, S.B., Chien, C.B., Roehl, H., 2004. Axon sorting in the optic tract requires HSPG synthesis by ext2 (dackel) and extl3 (boxer). Neuron 44, 947–960.

Lin, L., Cheung, A.W., Chan, S.O., 2005. Chiasmatic neurons in the ventral diencephalon of mouse embryos—Changes in arrangement and heterogeneity in surface antigen expression. Brain Res. Dev. Brain Res. 158, 1–12.

Lipscomb, B.W., Treloar, H.B., Greer, C.A., 2002. Cell surface carbohydrates reveal heterogeneity in olfactory receptor cell axons in the mouse. Cell Tissue Res. 308, 7–17.

Lipscomb, B.W., Treloar, H.B., Klenoff, J., Greer, C.A., 2003. Cell surface carbohydrates and glomerular targeting of olfactory sensory neuron axons in the mouse. J. Comp. Neurol. 467, 22–31.

Long, H., Sabatier, C., Ma, L., Plump, A., Yuan, W., Ornitz, D.M., Tamada, A., Murakami, F., Goodman, C.S., Tessier-Lavigne, M., 2004. Conserved roles for Slit and Robo proteins in midline commissural axon guidance. Neuron 42, 213–223.

Lorenzini, C.G., Baldi, E., Bucherelli, C., Sacchetti, B., Tassoni, G., 1997. 2-Deoxy-D-galactose effects on passive avoidance memorization in the rat. Neurobiol. Learn. Mem. 68, 317–324.

Martin, P.T., Scott, L.J.C., Porter, B.E., Sanes, J.R., 1999. Distinct structures and functions of related pre- and postsynaptic carbohydrates at the mammalian neuromuscular junction. Mol. Cell. Neurosci. 13, 105–118.

Martin, L.V., Weston, S., West, A.K., Chuah, M.I., 2002. Nerve growth factor promotes olfactory axonal elongation. NeuroReport 13, 621–625.

Mileusnic, R., Rose, S.P., Lancashire, C., Bullock, S., 1995. Characterisation of antibodies specific for chick brain neural cell adhesion molecules which cause amnesia for a passive avoidance task. J. Neurochem. 64, 2598–2606.

Mollicone, R., Trojan, J., Oriol, R., 1985. Appearance of H and B antigens in primary sensory cells of the rat olfactory apparatus and inner ear. Brain Res. 349, 275–279.

Montag-Sallaz, M., Schachner, M., Montag, D., 2002. Misguided axonal projections, neural cell adhesion molecule 180 mRNA upregulation, and altered behavior in mice deficient for the close homolog of L1. Mol. Cell. Biol. 22, 7967–7981.

Murrey, H.E., Gama, C.I., Kalovidouris, S.A., Luo, W.I., Driggers, E.M., Porton, B., Hsieh-Wilson, L.C., 2006. Protein fucosylation regulates synapsin Ia/Ib expression and neuronal morphology in primary hippocampal neurons. Proc. Natl. Acad. Sci. U. S. A. 103, 21–26.

Nagao, H., Yoshihara, Y., Mitsui, S., Fujisawa, H., Mori, K., 2000. Two mirror-image sensory maps with domain organization in the mouse main olfactory bulb. NeuroReport 11, 3023–3027.

Parkhomovskiy, N., Kammesheidt, A., Martin, P.T., 2000. *N*-acetyllactosamine and the CT carbohydrate antigen mediate agrin-dependent activation of MuSK and acetylcholine receptor clustering in skeletal muscle. Mol. Cell. Neurosci. 15, 380–397.

Pasterkamp, R.J., De Winter, F., Holtmaat, A.J., Verhaagen, J., 1998. Evidence for a role of the chemorepellent semaphorin III and its receptor neuropilin-1 in the regeneration of primary olfactory axons. J. Neurosci. 18, 9962–9976.

Pays, L., Schwarting, G., 2000. Gal-NCAM is a differentially expressed marker for mature sensory neurons in the rat olfactory system. J. Neurobiol. 43, 173–185.

Potter, S.M., Zheng, C., Koos, D.S., Feinstein, P., Fraser, S.E., Mombaerts, P., 2001. Structure and emergence of specific olfactory glomeruli in the mouse. J. Neurosci. 21, 9713–9723.

Puche, A.C., Poirier, F., Hair, M., Bartlett, P.F., Key, B., 1996. Role of galectin-1 in the developing mouse olfactory system. Dev. Biol. 179, 274–287.

Puche, A.C., Bartlett, P.F., Key, B., 1997. Substrate-bound carbohydrates stimulate signal transduction and neurite outgrowth in an olfactory neuron cell line. NeuroReport 8, 3183–3188.

Ressler, K.J., Sullivan, S.L., Buck, L.B., 1994. Information coding in the olfactory system: evidence for a stereotyped and highly organized epitope map in the olfactory bulb. Cell 79, 1245–1255.

Rodriguez, I., Feinstein, P., Mombaerts, P., 1999. Variable patterns of axonal projections of sensory neurons in the mouse vomeronasal system. Cell 97, 199–208.

Sabatier, C., Plump, A.S., Le, M., Brose, K., Tamada, A., Murakami, F., Lee, E.Y., Tessier-Lavigne, M., 2004. The divergent Robo family protein rig-1/Robo3 is a negative regulator of slit responsiveness required for midline crossing by commissural axons. Cell 117, 157–169.

Salazar, I., Sanchez Quinteiro, P., 2003. Differential development of binding sites for four lectins in the vomeronasal system of juvenile mouse: from the sensory transduction site to the first relay stage. Brain Res. 979, 15–26.

Salazar, I., Sanchez Quinteiro, P., Lombardero, M., Cifuentes, J.M., 2001. Histochemical identification of carbohydrate moieties in the accessory olfactory bulb of the mouse using a panel of lectins. Chem. Senses 26, 645–652.

Schwarting, G.A., Crandall, J.E., 1991. Subsets of olfactory and vomeronasal sensory epithelial cells and axons revealed by monoclonal antibodies to carbohydrate antigens. Brain Res. 547, 239–248.

Schwarting, G.A., Deutsch, G., Gattey, D.M., Crandall, J.E., 1992. Glycoconjugates are stage- and position-specific cell surface molecules in the developing olfactory system, 2: unique carbohydrate antigens are topographic markers for selective projection patterns of olfactory axons. J. Neurobiol. 23, 130–142.

St John, J.A., Key, B., 2001. Chemically and morphologically identifiable glomeruli in the rat olfactory bulb. J. Comp. Neurol. 436, 497–507.

St John, J.A., Key, B., 2002. Heterogeneity in olfactory neurons in mouse revealed by differential expression of glycoconjugates. Histochem. J. 34, 281–289.

St John, J.A., Key, B., 2005. Olfactory marker protein modulates primary olfactory axon overshooting in the olfactory bulb. J. Comp. Neurol. 488, 61–69.

Storan, M.J., Magnaldo, T., Biol-N'Garagba, M.C., Zick, Y., Key, B., 2004. Expression and putative role of lactoseries carbohydrates present on NCAM in the rat primary olfactory pathway. J. Comp. Neurol. 475, 289–302.

Strotmann, J., Wanner, I., Helfrich, T., Beck, A., Breer, H., 1994a. Rostro-caudal patterning of receptor-expressing olfactory neurones in the rat nasal cavity. Cell Tissue Res. 278, 11–20.

Strotmann, J., Wanner, I., Helfrich, T., Beck, A., Meinken, C., Kubick, S., Breer, H., 1994b. Olfactory neurones expressing distinct odorant receptor subtypes are spatially segregated in the nasal neuroepithelium. Cell Tissue Res. 276, 429–438.

Tenne-Brown, J., Key, B., 1999. Errors in lamina growth of primary olfactory axons in the rat and mouse olfactory bulb. J. Comp. Neurol. 410, 20–30.

Treloar, H., Tomasiewicz, H., Magnuson, T., Key, B., 1997. The central pathway of primary olfactory axons is abnormal in mice lacking the N-CAM-180 isoform. J. Neurobiol. 32, 643–658.

Vassar, R., Ngai, J., Axel, R., 1993. Spatial segregation of odorant receptor expression in the mammalian olfactory epithelium. Cell 74, 309–318.

Vassar, R., Chao, S.K., Sitcheran, R., Nunez, J.M., Vosshall, L.B., Axel, R., 1994. Topographic organization of sensory projections to the olfactory bulb. Cell 79, 981–991.

Walz, A., Rodriguez, I., Mombaerts, P., 2002. Aberrant sensory innervation of the olfactory bulb in neuropilin-2 mutant mice. J. Neurosci. 22, 4025–4035.

Weinhold, B., Seidenfaden, R., Rockle, I., Muhlenhoff, M., Schertzinger, F., Conzelmann, S., Marth, J.D., Gerardy-Schahn, R., Hildebrandt, H., 2005.

Genetic ablation of polysialic acid causes severe neurodevelopmental defects rescued by deletion of the neural cell adhesion molecule. J. Biol. Chem. 280, 42971–42977.

Xia, B., Hoyte, K., Kammesheidt, A., Deerinck, T., Ellisman, M., Martin, P.T., 2002. Overexpression of the CT GalNAc transferase in skeletal muscle alters myofiber growth, neuromuscular structure, and laminin expression. Dev. Biol. 242, 58–73.

Yamamoto, F., McNeill, P.D., 1996. Amino acid residue at codon 268 determines both activity and nucleotide-sugar donor substrate specificity of human histo-blood group A and B transferases. J. Biol. Chem. 271, 10515–10520.

Yoshida-Noro, C., Heasman, J., Goldstong, K., Vickers, L., Wylie, C., 1999. Expression of the Lewis group carbohydrate antigens during *Xenopus* development. Glycobiology 9, 1323–1330.

Yoshihara, Y., Kawasaki, M., Tamada, A., Fujita, H., Hayashi, H., Kagamiyama, H., Mori, K., 1997. OCAM: a new member of the neural cell adhesion molecule family related to zone-to-zone projection of olfactory and vomeronasal axons. J. Neurosci. 17, 5830–5842.

Zheng, C., Feinstein, P., Bozza, T., Rodriguez, I., Mombaerts, P., 2000. Peripheral olfactory projections are differentially affected in mice deficient in a cyclic nucleotide-gated channel subunit. Neuron 26, 81–91.